

Supporting Information

Fluorescence-Raman dual-mode quantitative detection and imaging of small-molecule thiols in cell apoptosis with DNA- modified gold nanoflowers

Chenbiao Li^{a, b, c, d}, Peifang Chen^{a, b, c, d}, Imran Mahmood Khan^{a, b, c, d}, Zhouping Wang^{a, b, c, d, e}, Yin Zhang^e, Xiaoyuan Ma^{*}, ^{a, b, c, d}

^aState Key Laboratory of Food Science and Technology, Jiangnan University, Wuxi 214122, China

^bSchool of Food Science and Technology, Jiangnan University, Wuxi 214122, China

^cInternational Joint Laboratory on Food Safety, Jiangnan University, Wuxi 214122, China

^dCollaborative innovation center of food safety and quality control in Jiangsu Province, Jiangnan University, Wuxi 214122, China

^eKey Laboratory of Meat Processing of Sichuan, Chengdu University, Chengdu 610106, China

*Corresponding

Authors:

maxy@jiangnan.edu.cn

Table of contents

1. Supplementary Experiments

1.1 Chemicals and Materials

1.2 Instrumentation

1.3 Cytotoxicity of T-2 Toxin

1.4 Cytotoxicity of C2-C1-AuNFs

1.5 Study on Cell Uptake of C2-C1-AuNFs by ICP-MS

1.6 TEM Analysis of Cells Sections

1.7 Localization of C2-C1-AuNFs in Cells

1.8 Determination of Small-Molecule Thiols Content and GSH Content in Cells

1.9 Experiment of Polyacrylamide Gel Electrophoresis

2. Supplementary Discussion

2.1 Calculation of the Concentration of Gold Seeds and AuNFs

2.2 Quantification of the C1 Coverage on the AuNFs Surface

2.3 Quantification of the C2 Hybridization Rate on the AuNFs Surface

2.4 Calculation of the Limit of Detection (LOD) in Vitro

2.5 Calculation of the Limit of Detection (LOD) in Vivo

3. Supplementary Table

4. Supplementary Figures

1. Supplementary Experiments

1.1 Chemicals and Materials.

Chloroauric acid ($\text{HAuCl}_4 \cdot 3\text{H}_2\text{O}$), trisodium citrate ($\text{C}_6\text{H}_5\text{Na}_3\text{O}_7 \cdot 2\text{H}_2\text{O}$), sodium chloride (NaCl), Polyvinylpyrrolidone (PVP) were domestic analytical reagents. Tween-20, Dimethyl sulfoxide (DMSO) and GSH monoester (GSH-OEt) were purchased from Sigma-Aldrich (Shanghai, China). Cell-Penetrating Peptides (TAT) was purchased from Nanjing Peptide Industry Biotechnology Co., Ltd (China), and the sequence of TAT is CYRGRKKRRQRRR. Thiolated polyethylene glycol (mPEG-SH, Mw~5kDa) was purchased from JenKem Technology Co., Ltd (China). DMEM medium, RPMI-1640 medium and PBS buffer were purchased from Shanghai Thermo Fisher Scientific (China). Fetal bovine serum and trypsin-EDTA were purchased from Thermo Fisher Scientific Co., Ltd (Waltham, MA, USA). DAPI Stain Solution was purchased from Nanjing Formax Biotechnology Co., Ltd (China). DNase I and Glutaraldehyde fixative (2.5%) was purchased from Beijing Solarbio Biotechnology Co., Ltd (China). Typing thiol assay kit and reduced glutathione (GSH) assay kit were purchased from Nanjing Jiancheng Bioengineering Institute (China). N-ethylmaleimide (NEM) was purchased from Shanghai Macklin Biochemical Co., Ltd (China). HeLa and HepG2 were purchased from Shanghai Institute of Biochemistry and Cell Biology, Chinese Academy of Sciences. QSG-7701, Calcein AM Cell Viability Assay Kit (CCK-F) and Propidium Iodide (PI) were purchased from Beyotime Biotechnology Corporation (China). GSH, Cell Counting Kit-8(CCK-8), Oligonucleotides, and RnaseA were purchased by Shanghai Sangon Biological Engineering Technology &

Services Co. Ltd (China). All chemicals were of analytical reagent grade and used as received unless specifically stated. Nucleic acid sequences are given as follows:

Chain1(C1):5'-SH-AAAAAAAAATAGTTTCTACTATCCAGCCTCGAGCGA-3';

Chain2(C2):5'-TCGCTCGAGGCTGGA/HS-SH/GGAAACTATAAAA-Cy5-3'

1.2 Instrumentation

JEM-2100 HR transmission electron microscope, 200 kV working voltage, JEOL Ltd, Japan; JEM-1010 transmission electron microscope, 80 kV working voltage, JEOL Ltd, Japan; UV-1800 ultraviolet spectrophotometer, Shimadzu Corporation, Japan; F-7000 fluorescence spectrometer, HITACHI, Japan; Laser confocal microscope, Zeiss, Germany; automatic cell counter, Shanghai Sixin Biotechnology Co., Ltd; DXR 2xi Raman Microscope Imaging Spectrometer, Thermo Fisher Scientific Inc.; Carbon dioxide thermostat cell incubator, Thermo Company, USA; SDirect-Q3 ultra-pure Water preparation instrument, Millipore, USA. SpectraMax M5/M5e microplate reader, the United States Molecular Devices; NexION 350D inductively coupled plasma mass spectrometer, PerkinElmer, US; Micropipette and Centrifuge 5424R desktop high-speed refrigerated centrifuge, Eppendorf, Germany; SZCL-2A digital display intelligent temperature control magnetic stirrer, Hangzhou Ruijia Precision Scientific Instrument Co., Ltd.; FLS 980 fluorescence spectrophotometer, Britain Edinburgh instruments; ZQZY-70B shaking incubator, Shanghai Zhichu Instrument Co., Ltd.; Constant temperature water bath, Shanghai Jinghong Experimental Equipment Company; Milli-Q device (18.2 MΩ, Millipore, Molsheim, France).

1.3 Cytotoxicity of T-2 Toxin

The CCK-8 method was used to determine the optimal concentration of T-2 toxin co-cultured with cells. The T-2 toxin was diluted with cell culture medium to different concentrations. HeLa cells were seeded in a 96-well plate at a density of 5000 cells per well. After culturing in incubator for 24 h (37°C, 5% CO₂), 10 µL of different concentrations of T-2 toxin were added to each well, so that the final concentration of T-2 toxin was 2 nM, 4 nM, 6 nM, 8 nM, 10 nM, 20 nM, 30 nM, 40 nM. After culturing for another 12 h, 10 µL of CCK-8 solution was added to each well. After 4 h incubation, the absorbance at 450nm was measured. The following formula was used to calculate the relative cell survival rate: relative cell survival rate = (experimental group absorbance value-blank group absorbance value) / (control group experimental value-blank group absorbance value) × 100%.

1.4 Cytotoxicity of C2-C1-AuNFs

HeLa cells were seeded in fluorescent plate (5000 cells/well). After 12 h, the culture medium was removed, and culture medium containing different concentrations of C2-C1-AuNFs was added, and the culture was continued for different periods of time. Then the medium was discarded and the cells were washed with PBS buffer. Then 100 µL of CCK-F reagent was added to each well and the culture was continued for 30 min. The fluorescence intensity was measured at 494 nm (excitation) and 517 nm (emission). The untreated cells were used as a control, and the survival rate of the cells was calculated. CCK-F and propidium iodide (PI) were used as dyes, and the effect of cells incubated with 3 nM nanosensors for 24 h was detected using laser confocal microscope.

1.5 Study on Cell Uptake of C2-C1-AuNFs by ICP-MS

After the C2-C1-AuNFs was digested by aqua regia, the concentration was adjusted to enter ICP-MS analysis, and the quality response peak (CPS) was obtained. HeLa cells were inoculated into 6-well plates for adherent growth for 24 h, and then basic media containing different concentrations of C2-C1-AuNFs were added and incubated with cells for 1.5 h. After the media was discarded, cells were washed with PBS for several times, and trypsin was added to suspend the cells. After counting, HeLa cells were collected by centrifugation. Aqua regia was added to the digested cells. After overnight, the solution was diluted several times and analyzed by ICP-MS, and the amount of C2-C1-AuNFs taken up by the cells was calculated.

1.6 TEM Analysis of Cells Sections

HeLa cells were seeded in a petri dish and cultured for 24 h. Then added C2-C1-AuNFs into the well and incubated for another 1.5 h. The cells were washed with PBS, digested using 0.25% trypsin, centrifuged, and fixed with 2.5% glutaraldehyde at 4 °C overnight. Then, the cells were fixed with 1% osmium tetroxide for 2 h, dehydrated in gradient ethanol, and embedded in epoxy resin. Thin sections were obtained and collected on copper grids. The copper grids were observed using TEM.

1.7 Localization of C2-C1-AuNFs in Cells

First, HeLa cells were cultured for 24 h. Next, the cells were incubated with nanosensors at 37 °C in 5% CO₂ for 1.5 h, and then the cells were washed three times with PBS. Finally, HeLa cells were stained with DAPI for 10 min, and then fixed with 4% paraformaldehyde solution for 15 min. Fluorescence images and Z-scan imaging

were acquired on a confocal laser scanning microscope.

1.8 Determination of Small-Molecule Thiols Content and GSH Content in Cells

Hela cells were seeded in 6-well plate at a density of 5×10^5 cells/mL. After 24 h of incubation in cell incubator, the serum-free medium was changed, and T-2 toxin was added to the final concentration of 20 nM to incubate the cells for different times. The cells were trypsinized at each time point, collected by centrifugation and washed twice with PBS. The cell pellet was resuspended in 500 μ L PBS, and the cells were sonicated to release intracellular components. Then GSH and small molecule thiols content were tested according to the kit instructions.

1.9 Experiment of Polyacrylamide Gel Electrophoresis

A 15% non-denaturing polyacrylamide gel was prepared, placed in the electrophoresis tank, and 1 \times TAE electrophoresis buffer was added. 2 μ L sample (1 μ M) was mixed with 2 μ L loading buffer, and then carefully added to the spotting hole. The voltage and electrophoresis time were set to 150 V and 30 min, respectively. After the electrophoresis, the gel was carefully removed, and stained in Gel Red staining solution for 5 min before taking pictures.

2. Supplementary Discussion

2.1 Calculation of the Concentration of Gold Seeds and AuNFs

From the TEM image and inset in Figure S1, the average particle size of the gold seed is 16 nm. Then we calculated the concentration of gold seeds according to the reported formula, where ϵ_{450} is the molar decadic extinction coefficient at $\lambda = 450$ nm and n is the dilution factor.

$$c(\text{gold seeds}) = \frac{A_{450}}{\epsilon_{450}} = \frac{0.514}{2.67 \cdot 10^8} = 1.93 \text{ nM}$$

AuNFs are synthesized by seed growth method. Gold seeds are used as the core for the growth of clade. According to reports and TEM pictures, all gold seeds are transformed into AuNFs. According to the law of conservation, the concentration of AuNFs in the solution after the reaction can be calculated.

$$c(\text{AuNSs}) = \frac{c(\text{gold seeds}) \cdot V(\text{gold seeds})}{V(\text{total})} = \frac{1.93 \text{ nM} \cdot 500 \mu\text{L}}{2600 \mu\text{L}} = 0.37 \text{ nM}$$

After centrifugation and purification, the concentration of AuNFs was adjusted to 4 nM and stored at 4 °C for further use.

2.2 Quantification of the C1 Coverage on the AuNFs Surface.

Before AuNFs were added, the UV-vis absorption spectra of C1 solutions of different concentrations were obtained (Figure S4). According to Lambert-Beer law, the absorbance at 260 nm is proportional to the concentration, and the slope is the product of the molar absorption coefficient (ϵ) and the thickness (b) of the liquid layer. Figure S4 shows that the regression equation is:

$$y=0.24 \cdot x, \quad R^2=0.9999$$

Where R^2 is the correlation coefficient. The change in the concentration of C1 was calculated from the changes in the absorbance values before and after the AuNFs were incubated together, and then the amount of C1 on the surface of each AuNFs particle was calculated.

$$\Delta C(C1) = \frac{\Delta A}{\epsilon b} = \frac{0.317}{0.23915} \mu M = 1.33 \mu M$$

The amount of C1 on the surface of per AuNFs particle:

$$N(C1/AuNFs) = \frac{\Delta C(C1) \cdot V(total)}{C(AuNFs) \cdot V(AuNFs)} = \frac{1.33 \mu M \cdot 200 \mu L}{4 nM \cdot 100 \mu L} = 662.77 C1/AuNF$$

2.3 Quantification of the C2 Hybridization Rate on the AuNFs Surface.

First, the fluorescence spectra of C2 solutions with different concentrations were obtained (Figure S5). The fluorescence intensity at 665 nm is proportional to the concentration. Figure S5 shows that the regression equation is:

$$y = 88264.65 \cdot x + 7271.17, \quad R^2 = 0.9910$$

The change in the concentration of C2 was calculated from the changes in the fluorescence intensity before and after C1-AuNFs were incubated together, and then the amount of C2 on the surface of each C1-AuNFs particle was calculated.

$$\Delta C(C2) = \frac{\Delta FI - a}{b} = \frac{48058 - 7271.17}{88264.65} \mu M = 0.46 \mu M$$

Δ_{FI} is the fluorescence difference before and after incubation with C1-AuNFs. The amount of C2 on the surface of per AuNF particle:

$$N(C2/AuNFs) = \frac{\Delta C(C2) \cdot V(total)}{C(AuNFs) \cdot V(AuNFs)} = \frac{0.46 \mu M \cdot 105 \mu L}{1 nM \cdot 100 \mu L} = 485.21 C2/AuNF$$

Hybridization rate (α) can be calculated:

$$\alpha = \frac{N(C2/AuNFs)}{N(C1/AuNFs)} \cdot 100\% = \frac{485.21}{622.77} \cdot 100\% = 77.91\%$$

2.4 Calculation of the Limit of Detection (LOD) in Vitro

The LOD was calculated with a sensitivity analysis. The calibration curve was plotted as: $y = a \cdot X + b$, where **a** and **b** are the variables obtained with a least-squares linear regression of the signal-concentration curve, with variable **y** representing the fluorescence intensity or the SERS intensity at a GSH concentration of **X** (mM).

When $a > 0$

$$LOD = \frac{(C_{blank} + 3\delta) - b}{a}$$

When $a < 0$

$$LOD = \frac{(C_{blank} - 3\delta) - b}{a}$$

where δ is the standard deviation and C_{blank} is the SERS or fluorescence intensity of the blank sample (without GSH).

2.5 Calculation of the Limit of Detection (LOD) in Vivo

LOD for intracellular quantification was calculated according to ICHQ2B guidelines.^{1,2} It is expressed as: $LOD = 3.3 \delta / S$. Where δ is the standard deviation of the response value, and the standard deviation of the y-intercept of the regression line is taken as δ . S is the slope of the calibration curve.

3. Supplementary Table

Table S1. Fluorescence lifetime of Cy5 and C2-C1-AuNFs.

	B ₁	T ₁ /ns	B ₂	T ₂ /ns	T/ns
C2-C1	3799.98	9.65	1.35	151.32	10.44
C2-C1-AuNFs	3451.28	7.44	1.12	107.48	7.91

Table S2. Raman Bands of Typical Vibrational Modes of Cy5

Raman bands (cm⁻¹)	Assignments of Cy5
1045	alkane chain linker
1140	C-H in-plane bending
1217	C-N stretching
1268	C-N-C symmetric stretching
1361	CH ₂ in-plane deformation
1405	CH ₃ symmetric deformation
1468	C=C, ring-stretching
1595	C=N stretching vibration

Table S3. Comparison of Different Methods for the Detection of Small-Molecule Thiols/GSH

Detect method	Sensing element or mechanism	Dynamic linear range	LOD	Intracellular imaging	Refs
Turn-on fluorescence	GSH can replace the TPdye-embedded hairpin-DNA off the AgNP surface, turning on the fluorescence of the TPdyes.	1 μ M-10 μ M	0.3 μ M	√	3
Turn-on fluorescence	The fluorescence intensity of CDs was significantly reduced by adding Hg ²⁺ , when GSH was added, their complexation with metal ions could restore the fluorescence intensity.	16.7 μ M-100 μ M	3.6 μ M	√	4
Turn-on fluorescence	The reduction of the phenanthroline N^N donor by GSH may influence the MLCT state of the iridium (III) complex.	0.2 M-2 M	1.67 μ M	√	5
Turn-on fluorescence	A NIR fluorescent probe possessed three potential reaction sites for facilitating simultaneous recognition of biothiols by yield different products with distinct signal outputs	0 μ M-250 μ M	2.596 μ M	√	6
Turn-on SERS	GSH cleaves the disulfide bond in SPDP, thereby enhancing the SERS signal of SPDP.	10 nM-500 nM	0.01 μ M		7
Turn-off SERS	GSH cleaves the disulfide bond in PEDA, resulting in a signal-off SERS response.	0 μ M-1 μ M	0.25 μ M		8
Chemiluminescence	Small molecule thiols mediated the cleavage of sulfonate bond and triggered the chemically initiated electron exchange luminescence reaction.	0.5 μ M -100 μ M		√	9
Electrochemiluminescence	The DNAzyme amplification strategy driven by Mn ²⁺ is combined with the allosteric transformation triggered by DNA-walker.	1 μ M-200 μ M	0.44 μ M	√	10
Electrochemiluminescence	In the presence of GSH, effective redox reaction between manganese dioxide and GSH restores the ECL signal.	0.1 nM-1 μ M	0.03 nM		11
Aggregation-induced emission	After GSH breaks the disulfide bond, the TPE molecules fall off and aggregate, and then emit strong fluorescence.	1 nM-10 μ M	1 nM	√	12

Colorimetric	Ru@G exhibited superior peroxidase-like activity	1 μ M -60 μ M	0.54 μ M		13
Colorimetric	The Fe ₃ O ₄ @MIL-100(Fe) showed peroxidase- and catalase-like activities.	1 μ M-45 μ M	0.26 μ M		14
Turn-on fluorescence and Turn-off SERS	Disulfide bonds in DNA were cleaved by small-molecule thiols.	0.01-3 mM	1.454 μ M and 0.913 μ M	√	This work

4. Supplementary Figures

Fig. S1. (A) Absorption spectra and (B) TEM image of gold seeds; The inset is statistics of particle size distribution of gold seeds.

Fig. S2. Statistics of particle size distribution of AuNFs.

Fig. S3. Optimization of C1 concentration.

Fig. S4. The UV-vis absorption spectrum of C1 solution itself; The inset is linear fitting curve of absorbance and C1 concentration.

Fig. S5. Linear fitting curve of fluorescence intensity and C2 concentration.

Fig. S6. Optimization of C2 concentration with fluorescence intensity difference.

Fig. S7. Optimization of C2 concentration with Raman characterization.

Fig. S8. Transient fluorescence decays of C1-C2 and C1-C2-AuNFs.

Fig. S9. (A) SERS spectrum and (B) The Raman intensity at 1366 cm^{-1} obtained from 20 different spots.

Fig. S10. Stability of C2-C1-AuNFs in different concentrations of NaCl.

Fig. S11. Restriction digestion and GSH stability of C2-C1-AuNFs.

Fig. S12. Performance of C2-C1-AuNFs in different pH solutions.

Fig. S13. Stability of C2-C1-AuNFs in buffer or medium.

Fig. S14. Time Optimization for GSH reaction.

Fig. S15. (A) Verification of GSH shearing disulfide bond; (B) Agarose gel electrophoresis. Lane 1: C1, Lane 2: C2, lane 3: C1-C2 complementary double strand, lane 4: After C1-C2 complementary double strand reacts with GSH (The band of short chains containing Cy5 are diffuse and unclear, possibly because the chain has too few bases).

Fig. S16. CCK-8 result of T-2 toxin with different concentrations incubated with Hela cells for 12 h (The formula in B is the fitted equation).

Fig. S17. Evaluation of C2-C1-AuNFs cytotoxicity through fluorescence imaging; Scale bar = 20 μm .

Fig. S18. The linear relationship between the concentration of C2-C1-AuNFs and the mass response peak (CPS) obtained from ICP-MS.

Fig. S19. TEM image of C2-C1-AuNFs in Hela cells; Scale bar = 1 μm .

Fig. S20. (A) Localization of C2-C1-AuNFs inside cells; (B) 3D image of the C2-C1-AuNFs-incubated Hela cell; (C) Z-stack images of cells with C2-C1-AuNFs; The red channel is Cy5 fluorescence from activated C2-C1-AuNFs and the blue channel is DAPI for nucleus staining; Scale bar = 20 μm .

Fig. S21. Intracellular GSH induced fluorescence imaging validation; Scale bar = 40 μm .

Fig. S22. The effect of T-2 toxin treatment time on the Raman spectra of Hela cells.

Fig. S23. Raman spectroscopy detection in different cells after T-2 toxin stimulation for **(A)** 0 h or **(B)** 6 h.

References

- 1 M. Sarkar, S. Khandavilli and R. Panchagnula, *J. Chromatogr. B*, 2006, **830**, 349-354.
- 2 *International conference on harmonization, Geneva 1996 March*.
- 3 Q. Tang, N. N. Wang, F. L. Zhou, T. Deng, S. B. Zhang, J. S. Li, R. H. Yang, W. W. Zhong and W. H. Tan, *Chem. Commun.*, 2015, **51**, 16810-16812.
- 4 N. Zhou, Y. Shi, C. Sun, X. Zhang and W. Zhao, *Spectrochim Acta A Mol Biomol Spectrosc*, 2020, **228**, 117847.
- 5 Z. Mao, J. Liu, T. S. Kang, W. Wang, Q. B. Han, C. M. Wang, C. H. Leung and D. L. Ma, *Sci Technol Adv Mater*, 2016, **17**, 109-114.
- 6 Y. Yang, Y. Feng, H. Li, R. Shen, Y. Wang, X. Song, C. Cao, G. Zhang and W. Liu, *Sens. Actuators, B*, 2021, **333**.
- 7 C. Jiang, F. Huang, Y. Chen and L. Jiang, *Dalton Trans.*, 2021, DOI: 10.1039/d1dt01474a.
- 8 C. Wei, X. Liu, Y. Gao, Y. Wu, X. Guo, Y. Ying, Y. Wen and H. Yang, *Anal. Chem.*, 2018, **90**, 11333-11339.
- 9 A. Fu, Y. Mao, H. Wang and Z. Cao, *J Pharmaceut Biomed*, 2021, **204**, 114266.
- 10 J. J. Ge, Y. Zhao, X. S. Gao, H. K. Li and G. F. Jie, *Anal. Chem.*, 2019, **91**, 14117-14124.
- 11 J. Guo, M. Xie, P. Du, Y. Liu and X. Lu, *Anal. Chem.*, 2021, **93**, 10619-10626.
- 12 Y. H. Hu, X. P. Cao, Y. S. Guo, X. F. Zheng, D. J. Li, S. K. Chen, G. Chen and J. M. You, *Anal Bioanal Chem*, 2020, **412**, 7811-7817.
- 13 P. Keoingthong, Q. Hao, S. Li, L. Zhang, J. Xu, S. Wang, L. Chen, W. Tan and Z. Chen, *Chem. Commun.*, 2021, **57**, 7669-7672.
- 14 J. B. Xu, Y. Y. Xing, Y. T. Liu, M. Z. Liu and X. H. Hou, *Anal. Chim. Acta*, 2021, **1179**.

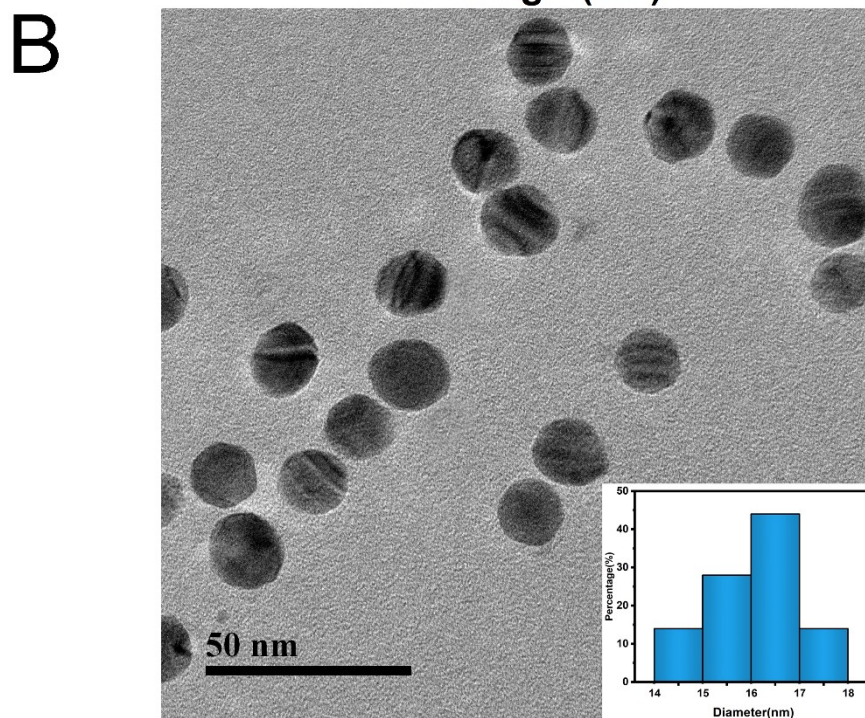
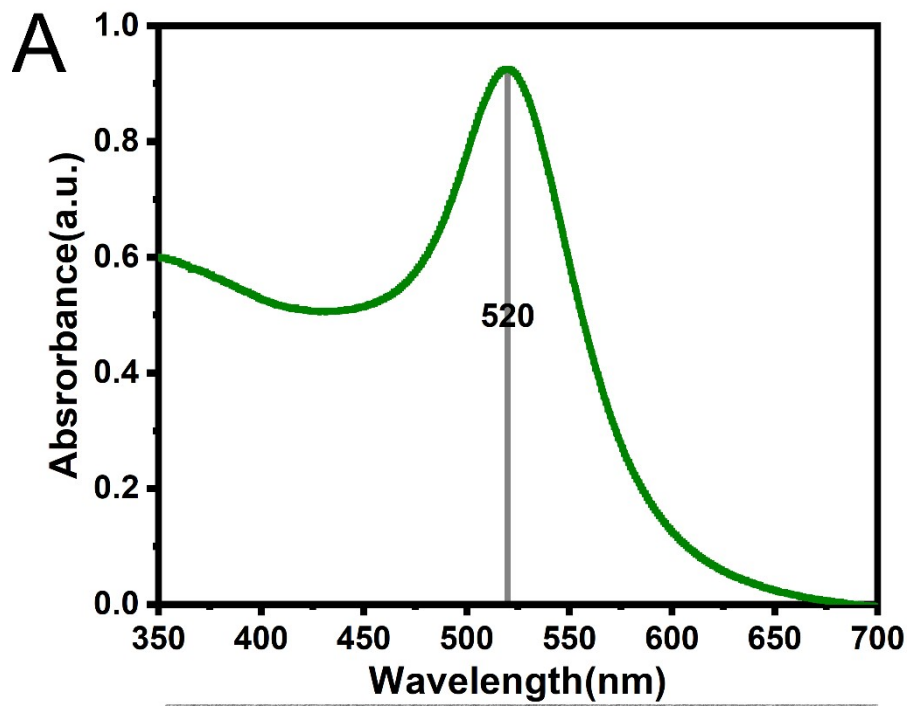


Fig. S1

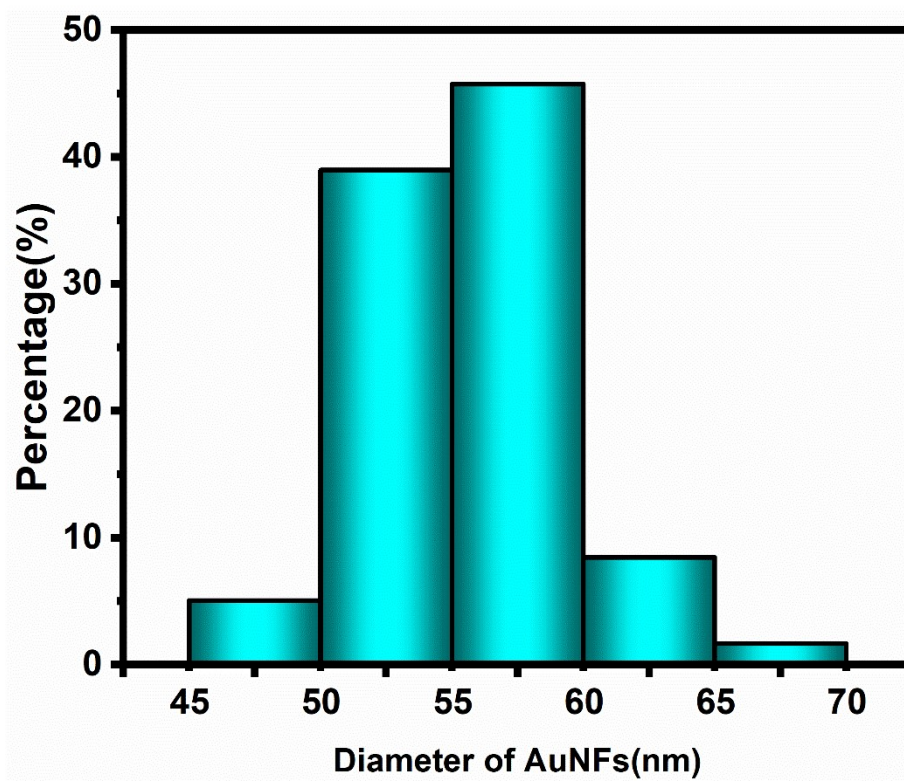


Fig. S2

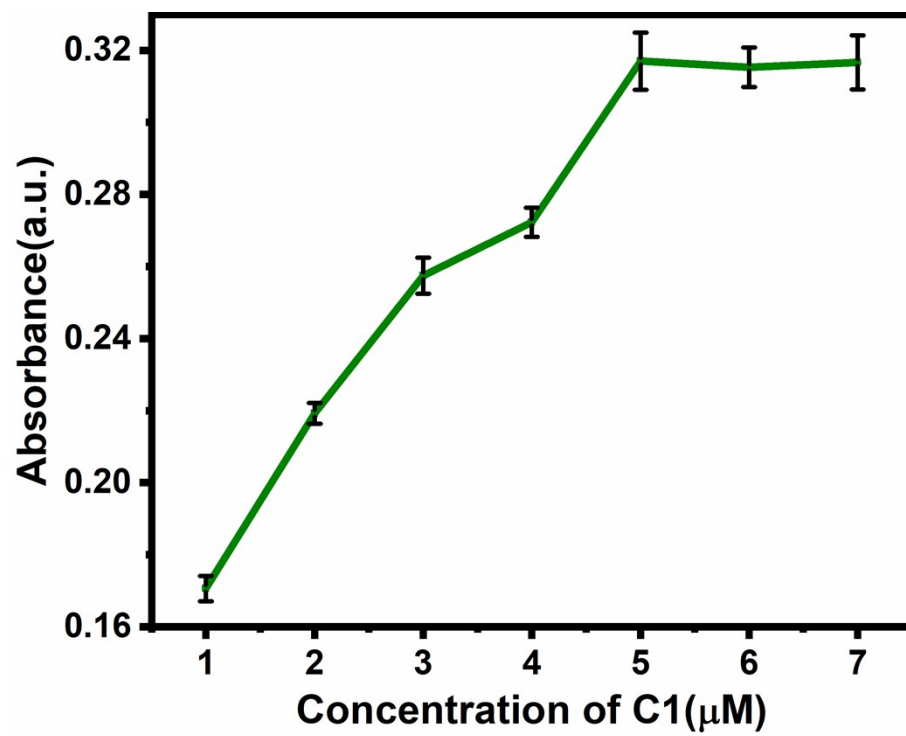


Fig. S3

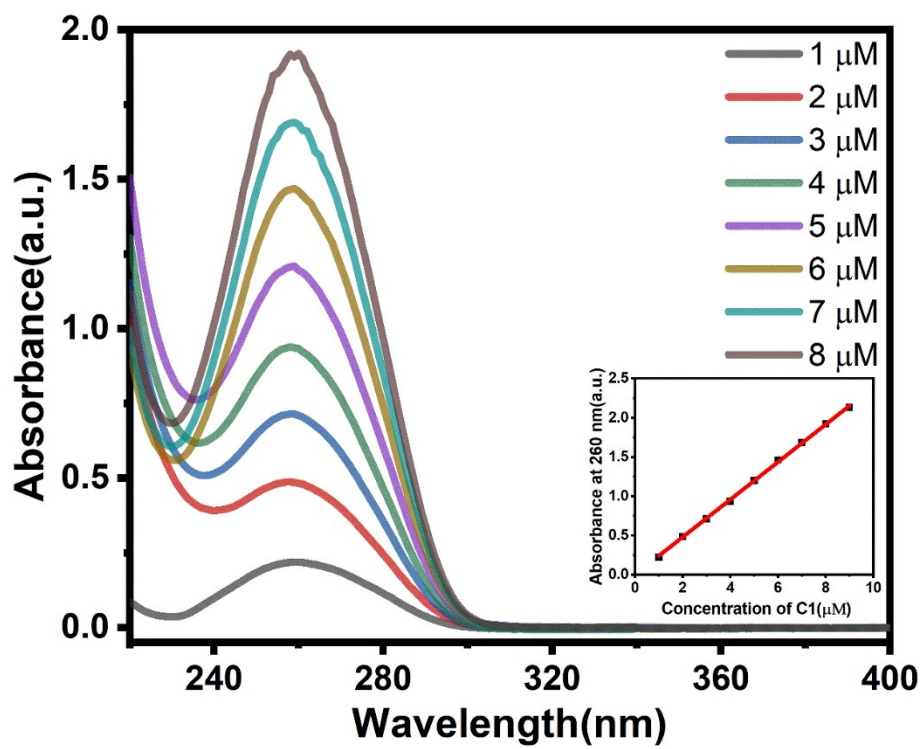


Fig. S4

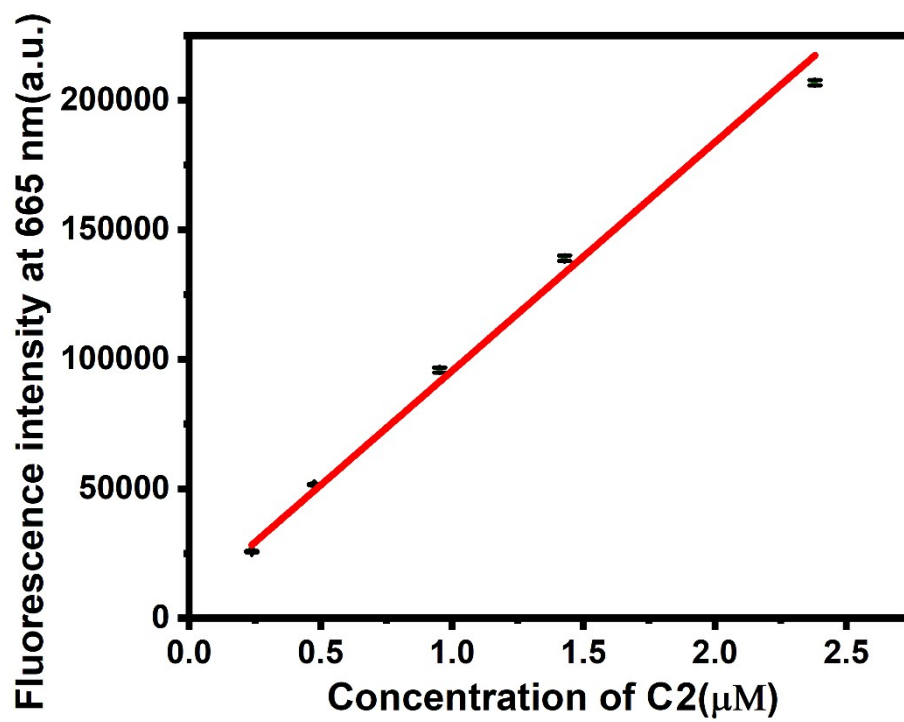


Fig. S5

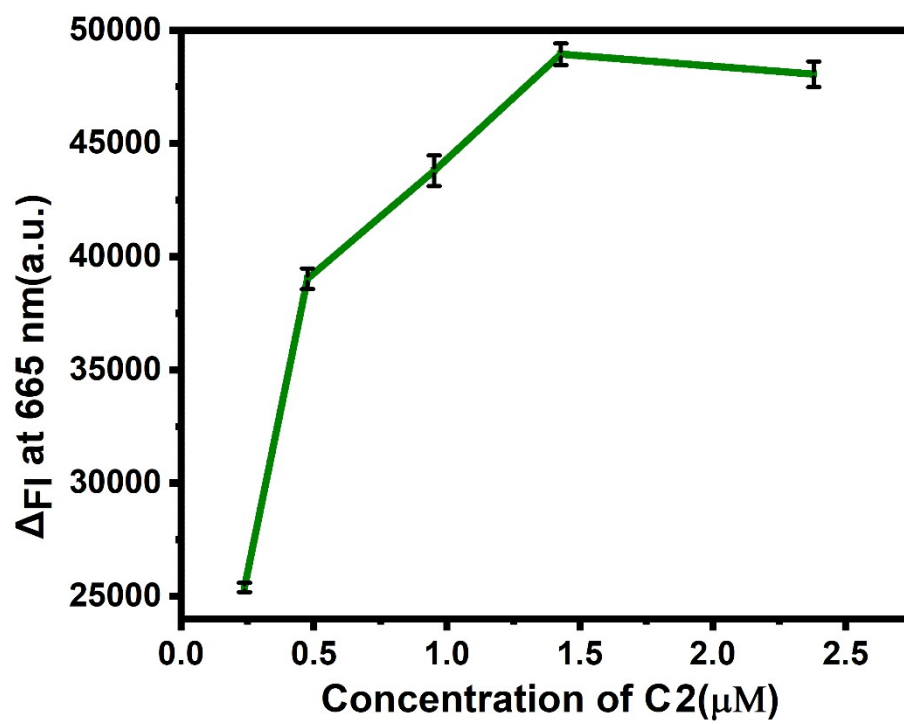


Fig. S6

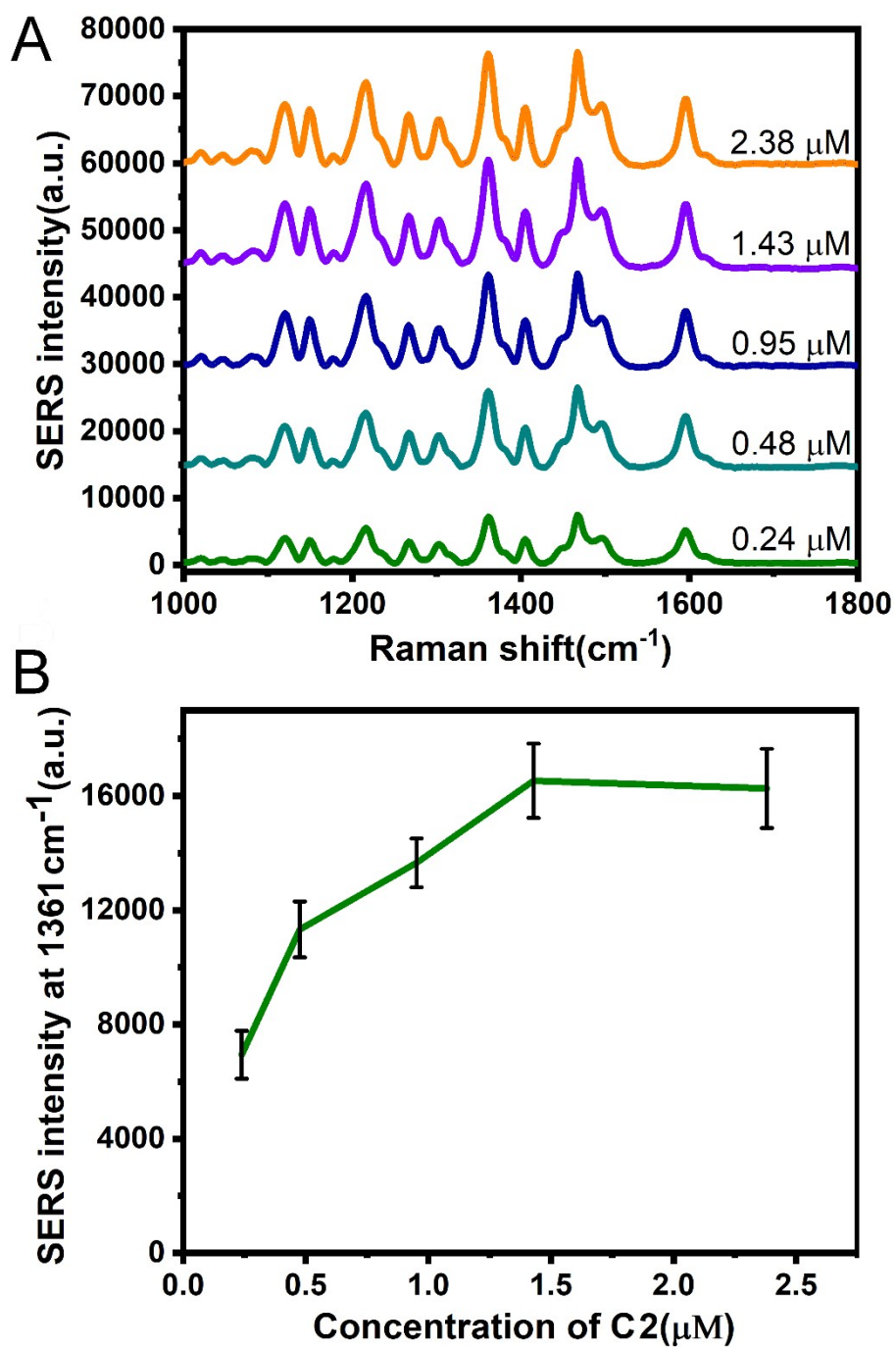


Fig. S7

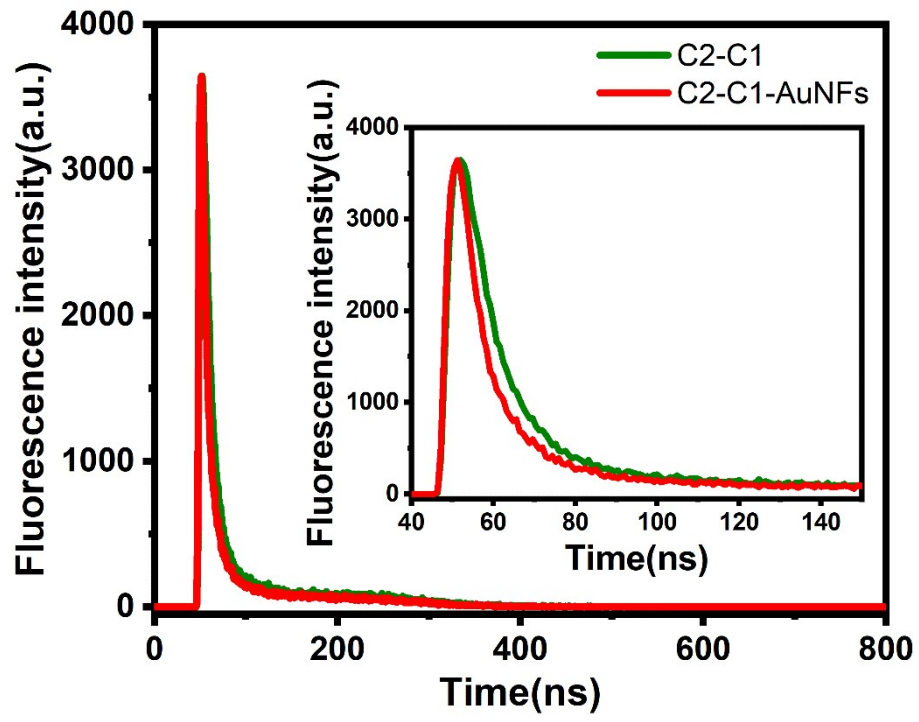


Fig. S8

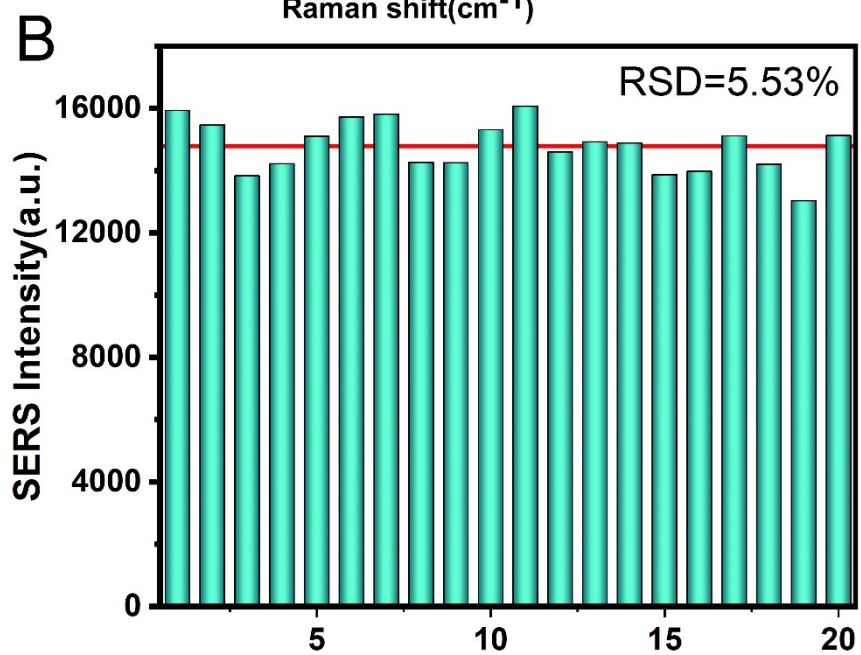
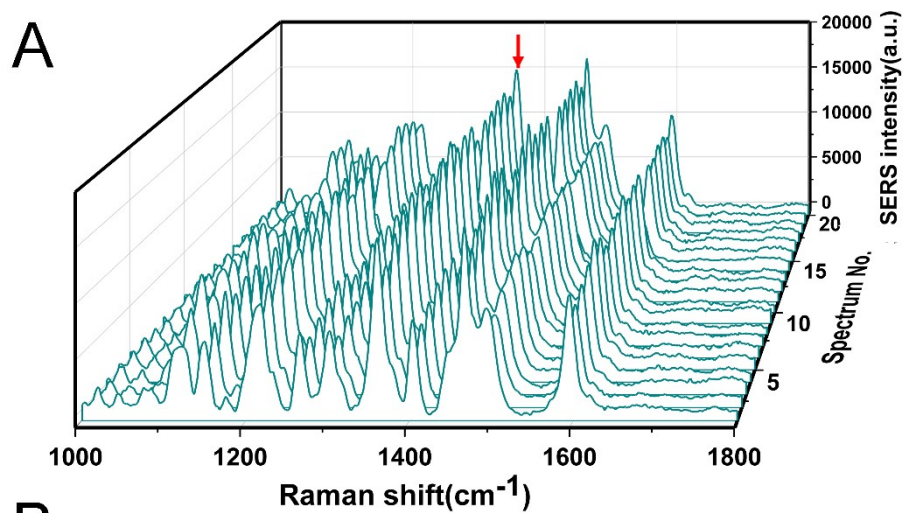


Fig. S9

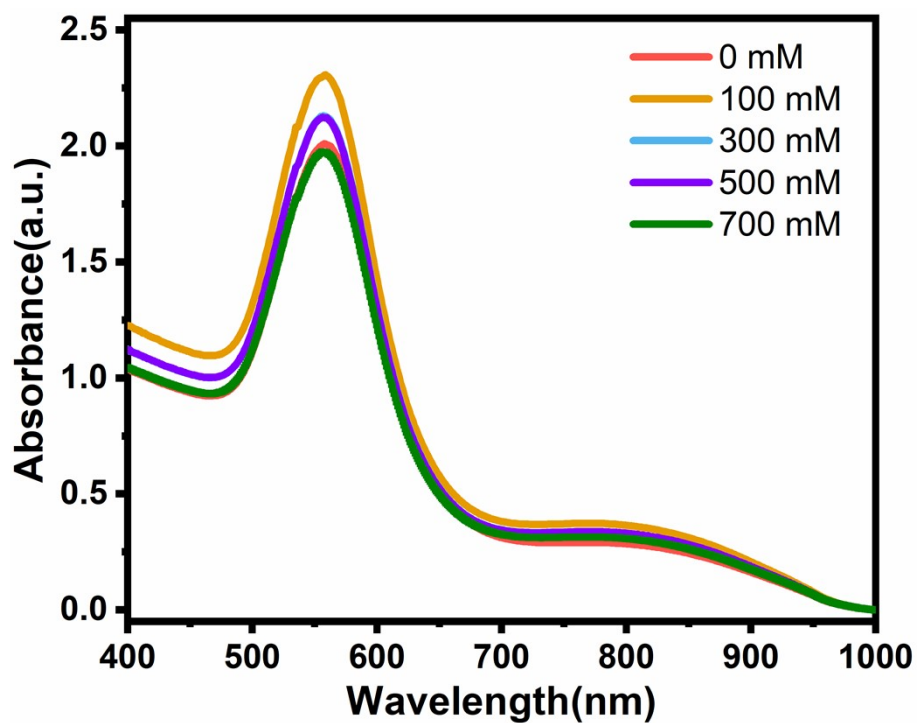


Fig. S10

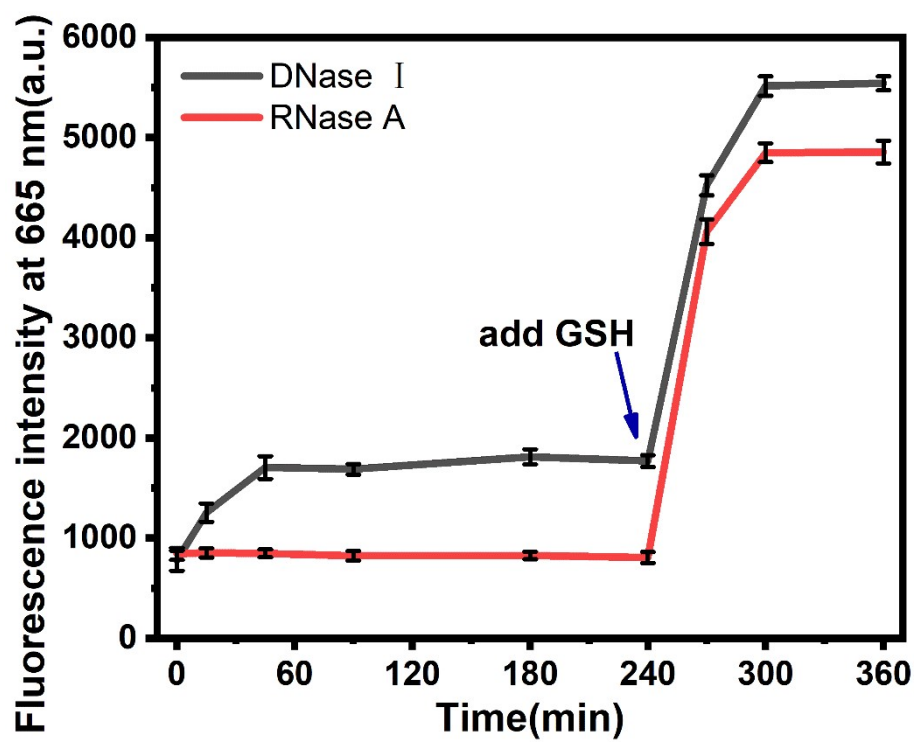


Fig. S11

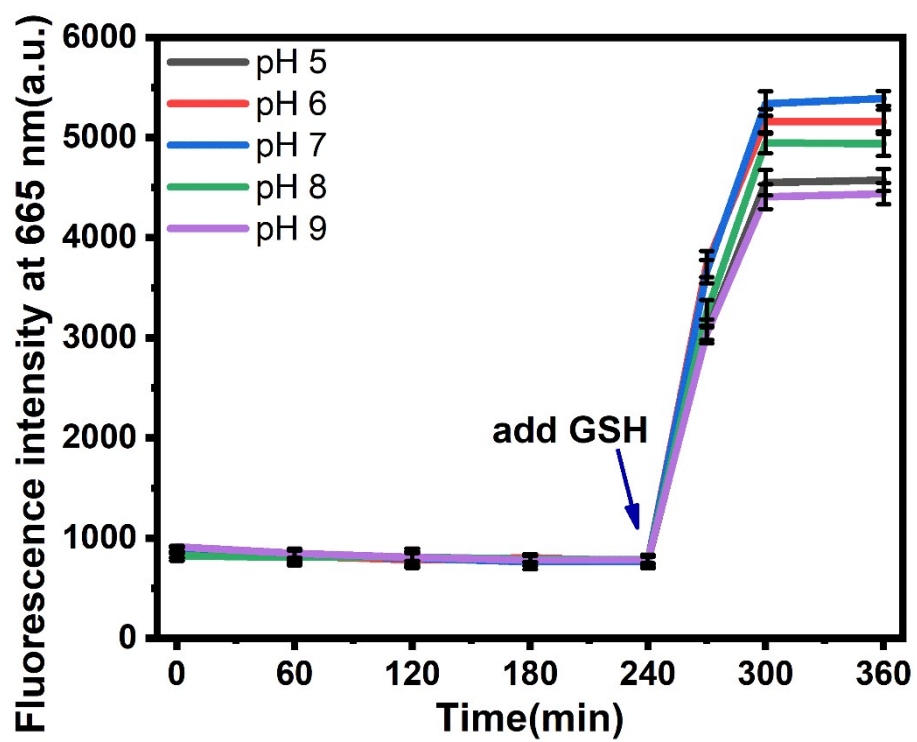


Fig. S12

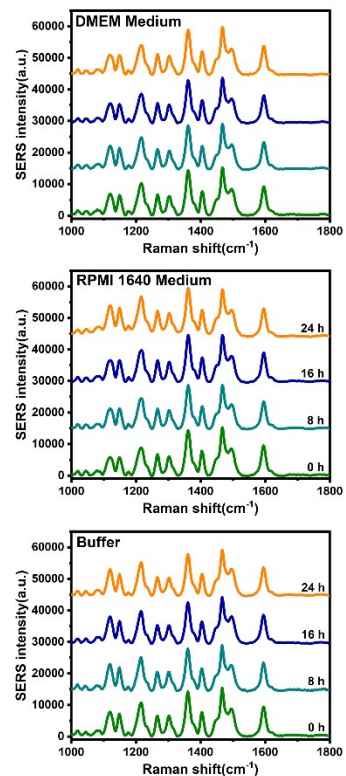
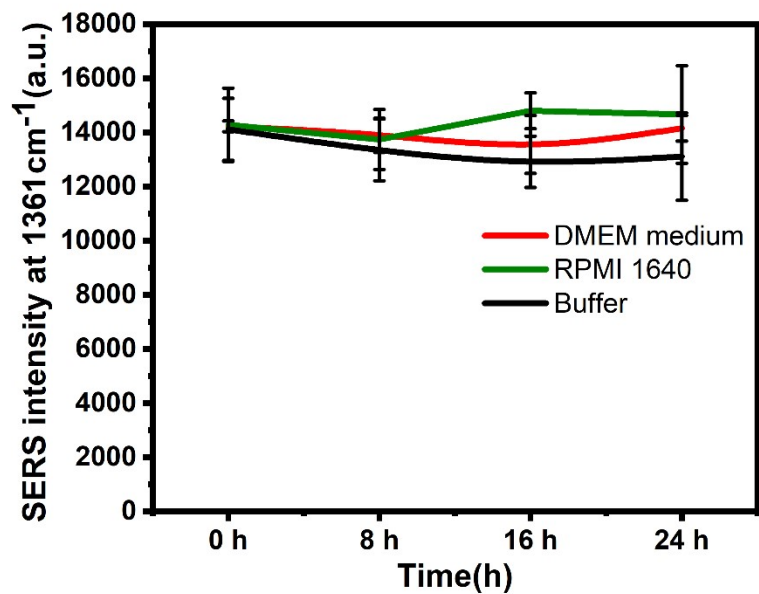


Fig. S13

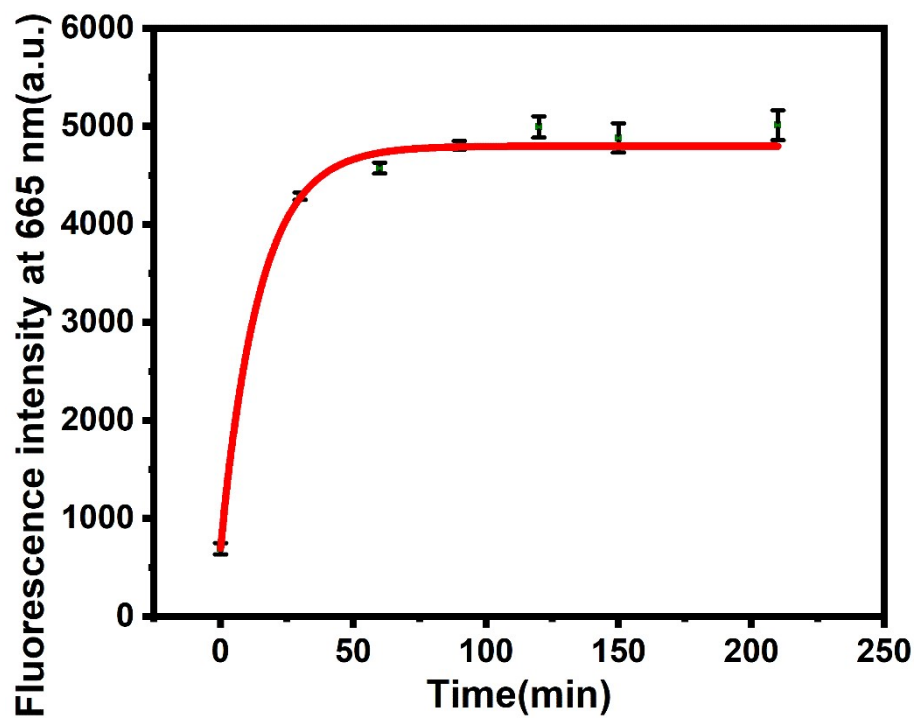


Fig. S14

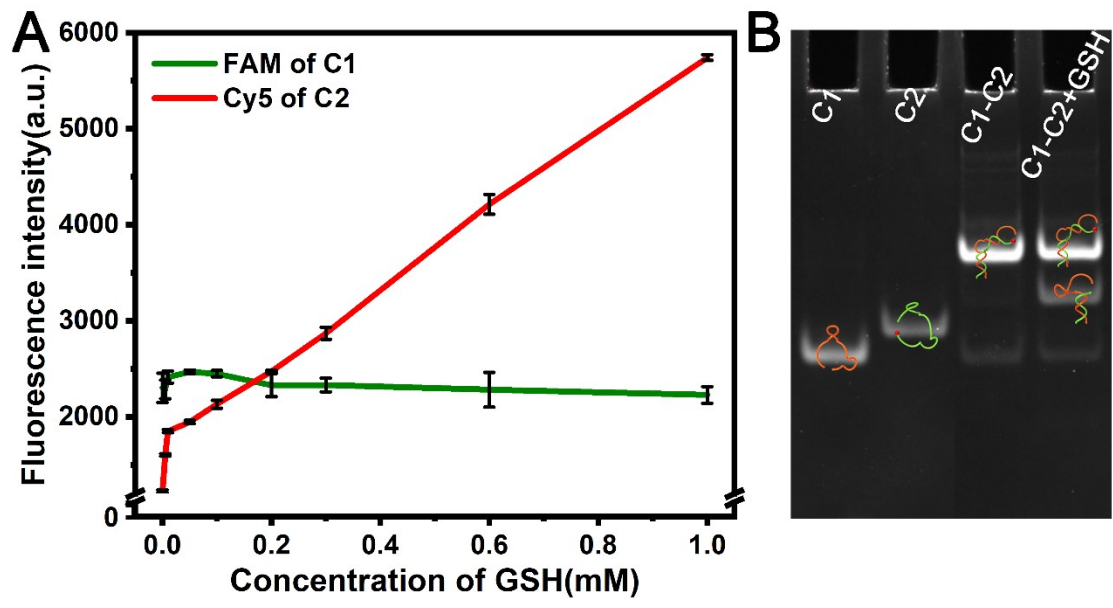


Fig. S15

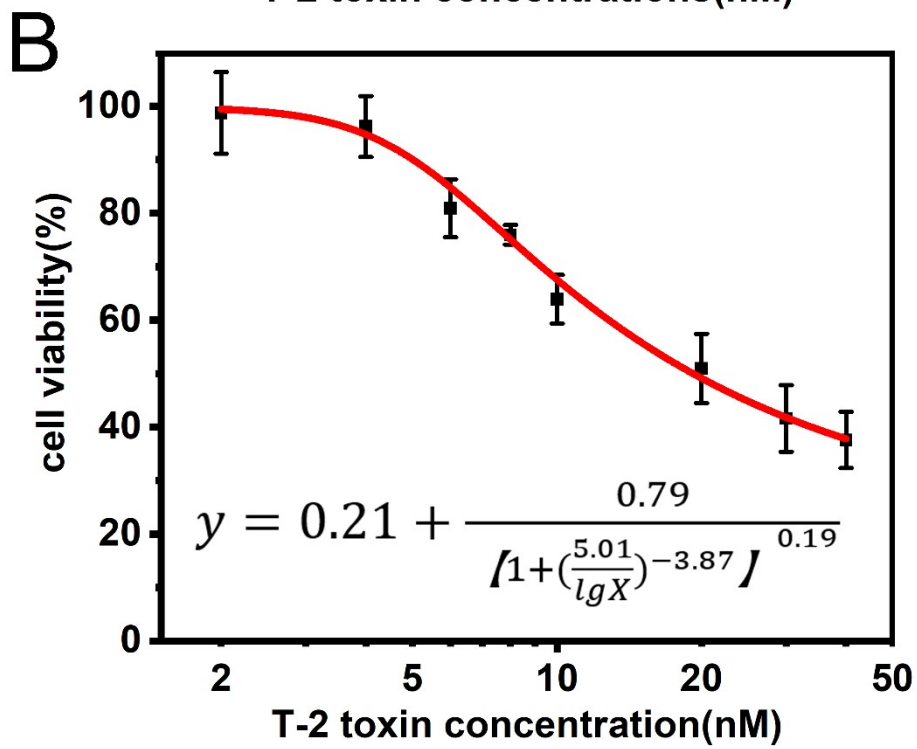
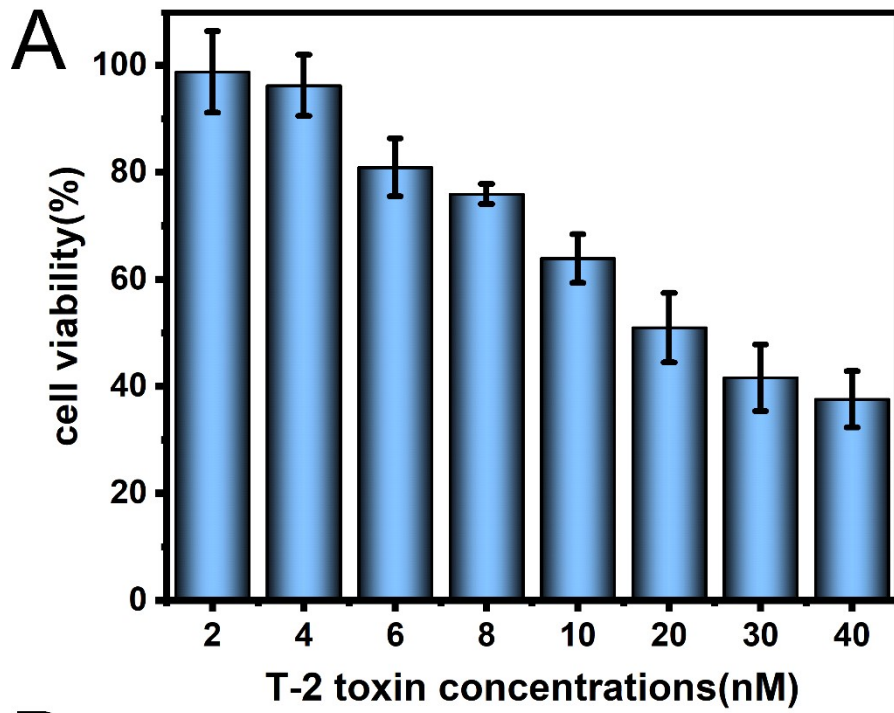


Fig. S16

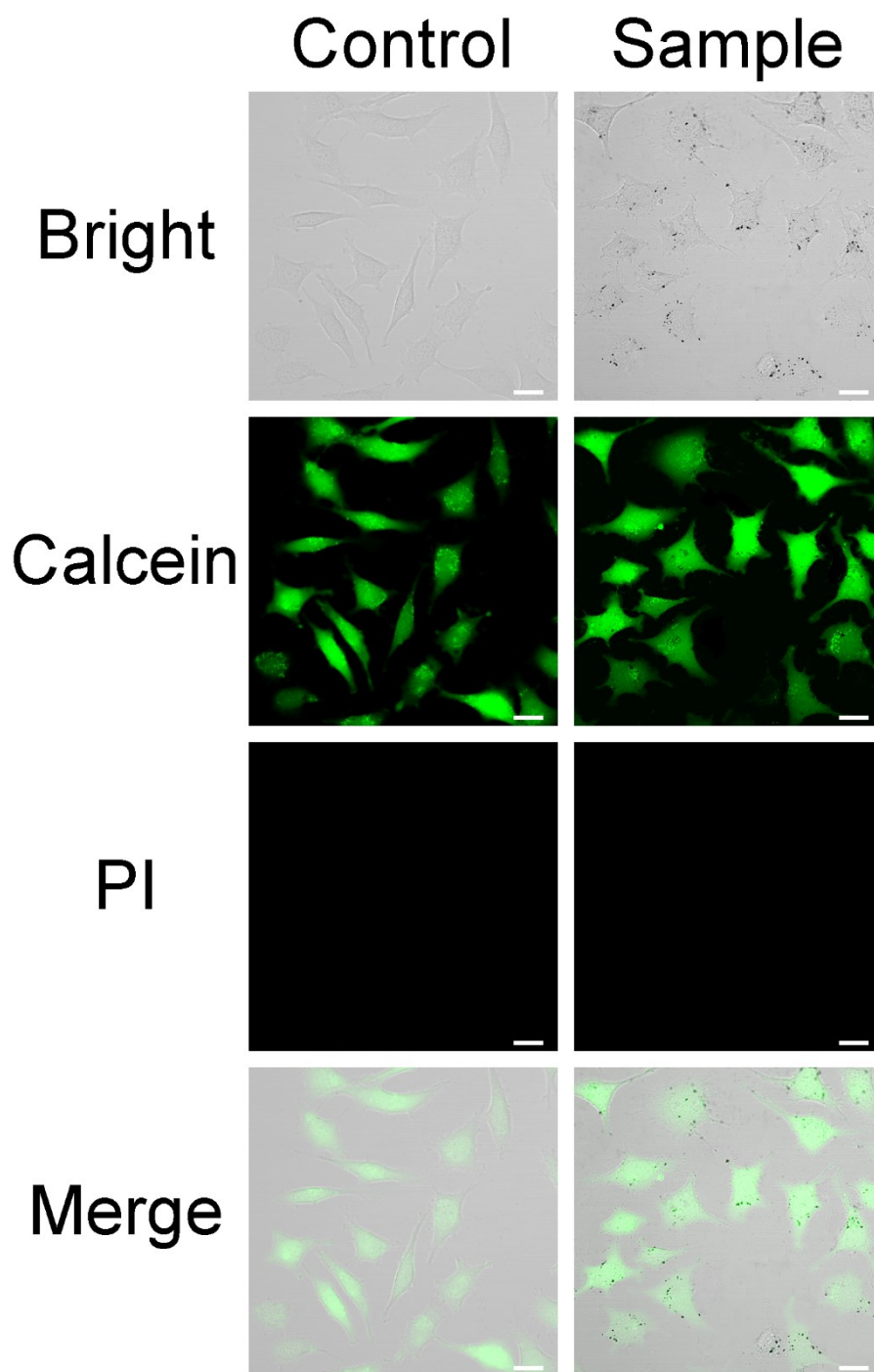


Fig. S17

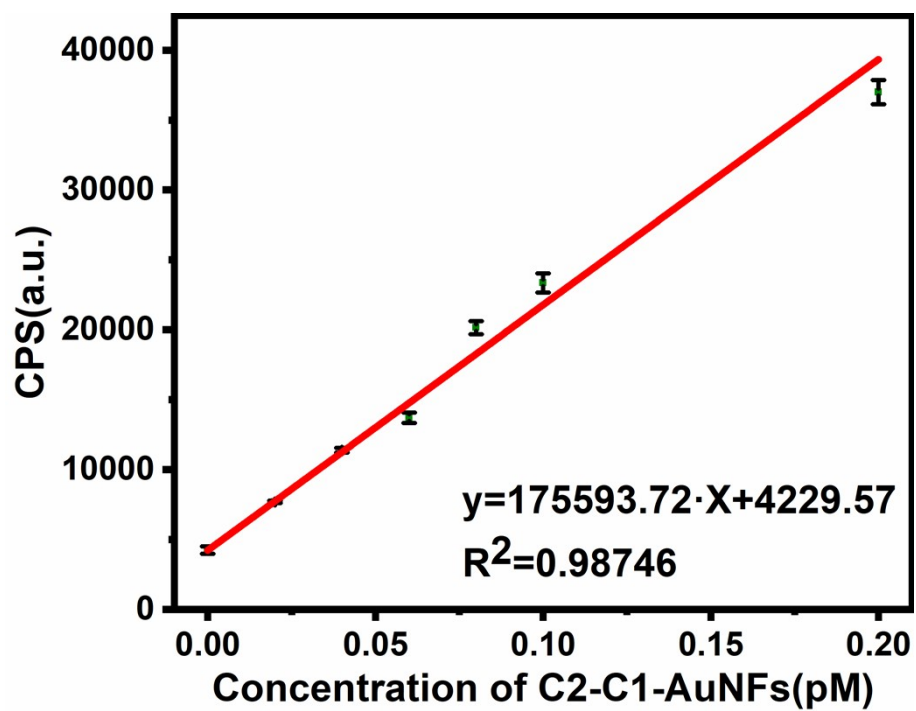


Fig. S18

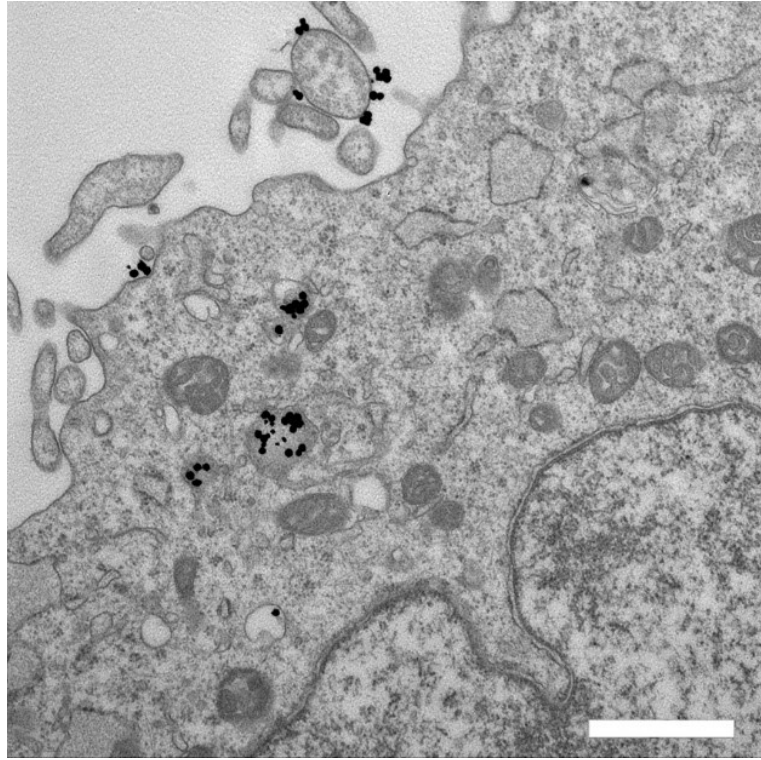


Fig. S19

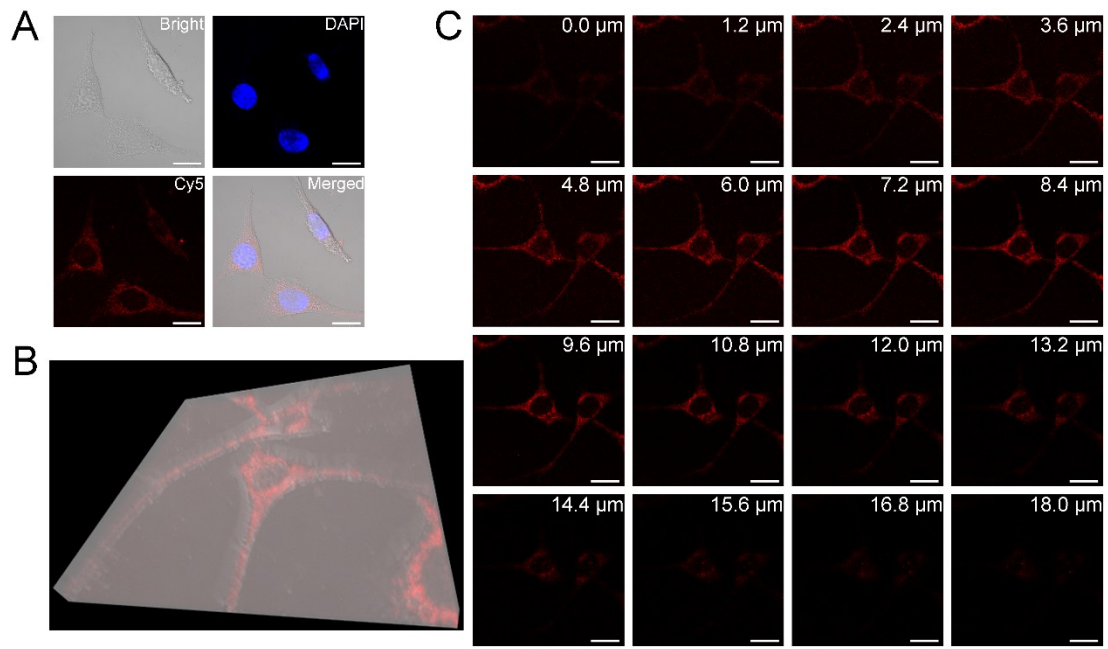


Fig. S20

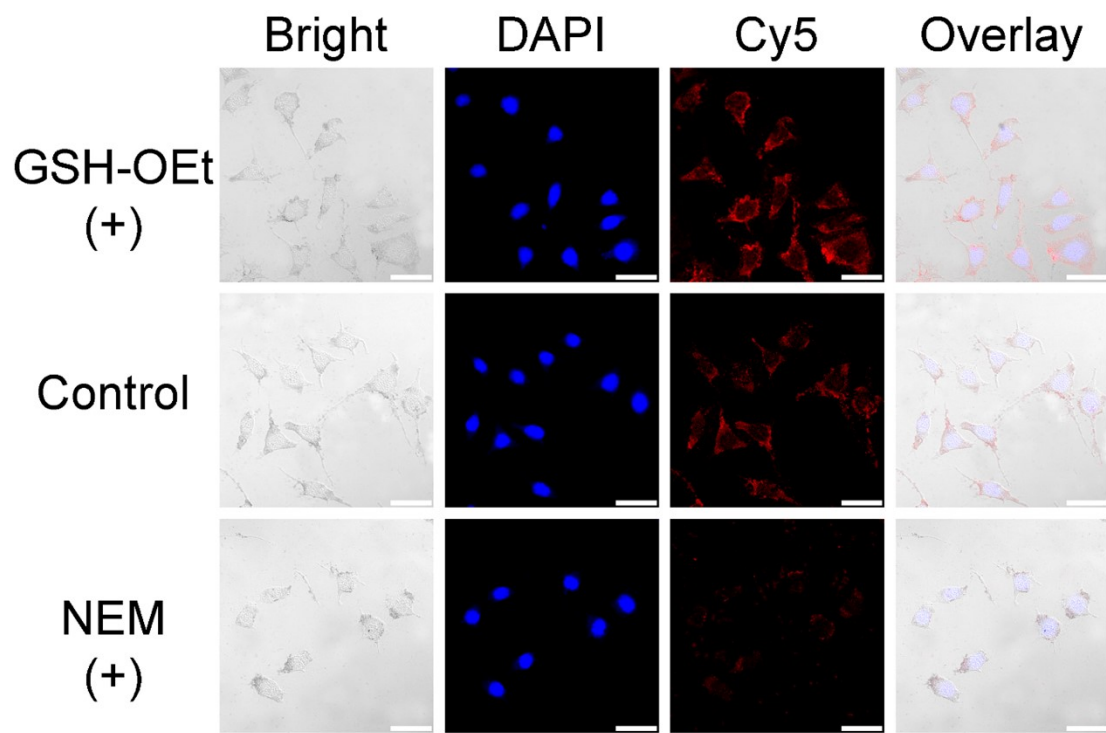


Fig. S21

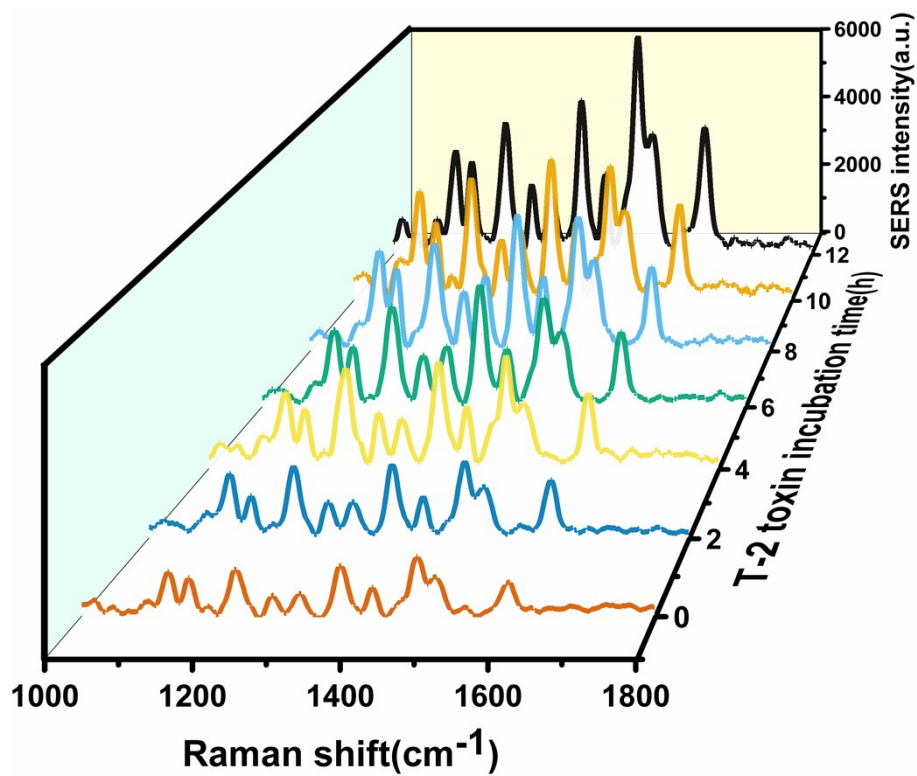


Fig. S22

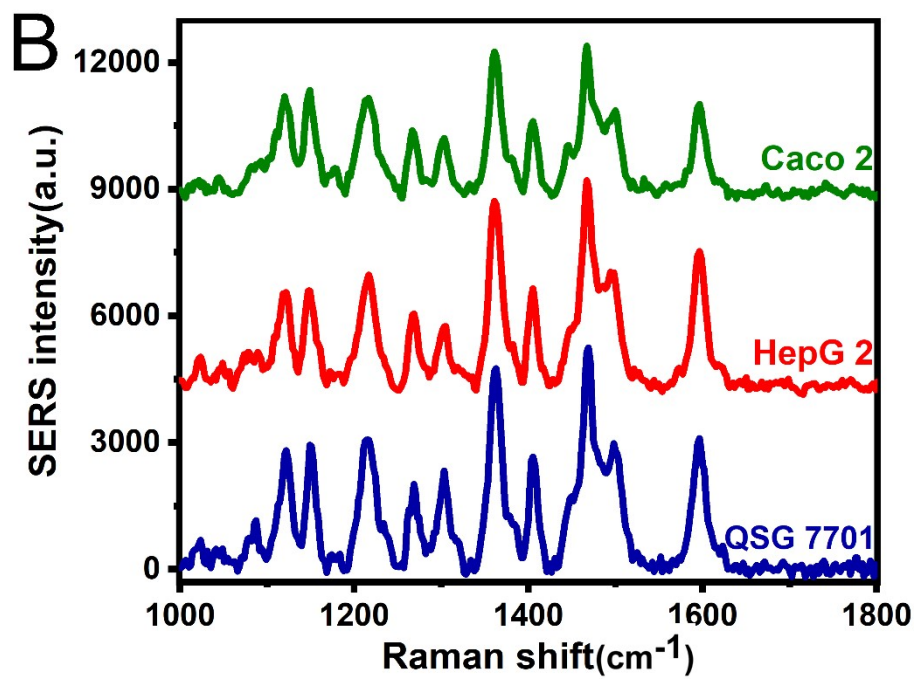
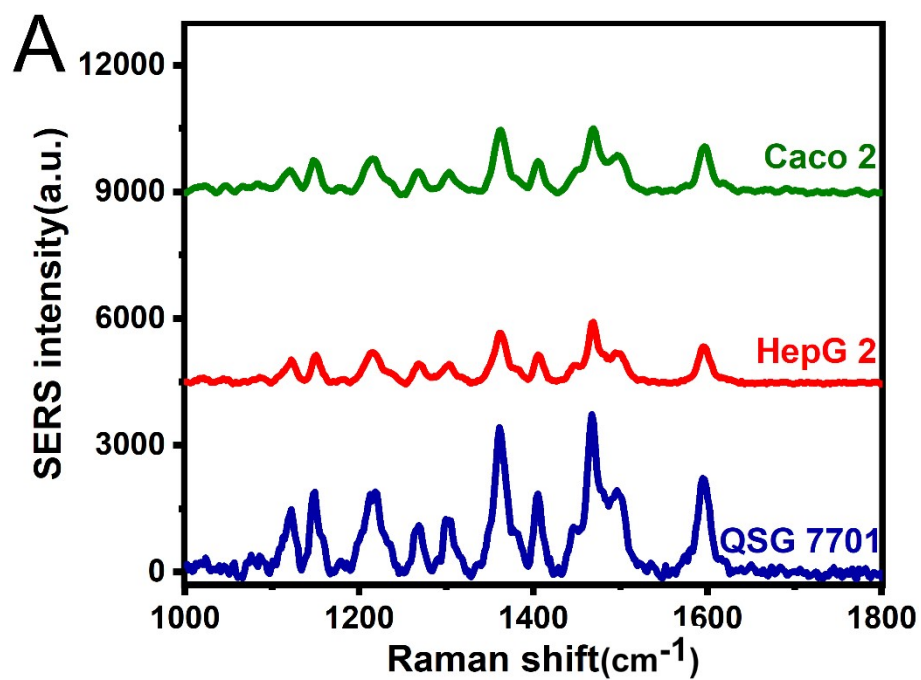


Fig. S23